Solar and Stellar Multi-scale Activity
Proceedings IAU Symposium No. 400, 2026
S. Vargas-Domínguez & J. C. Buitrago-Casas, eds.
doi:10.1017/S1743921326106929

Solar Flares from 1976–2025: GOES Analytics and SARIMAX / XGBoost Forecasts

Juan Camilo Buitrago-Casas[1] **and Andrea Lizeth López-Rodríguez**[2]

[1]Space Sciences Laboratory, University of California Berkeley
7 Gauss Way, 94720, Berkeley, USA
email: juan@berkeley.edu

[2]Observatorio Astronómico Nacional, Universidad Nacional de Colombia,
Carrera 45, Bogotá, 111321, Colombia
email: allopezro@unal.edu.co

Abstract. We analyze solar flares from 1976–2025 using the GOES/XRS_B event record to construct two monthly products: (i) counts of flares with peak flux $\geq$B1 and (ii) mean XRS_B flux, summarized as year×month heat-maps that separate *productivity* from *energetics*. We then pursue two complementary forecasting tracks. **(A) Annualized SARIMAX:** applying SARIMAX$(0, 0, 3) \times (1, 1, 1)_{11}$ to an *annual mean* series derived from daily counts improves over an annual naïve seasonal baseline (MSE = 2.37 vs. 4.93; MAE = 1.25 vs. 1.80), with diagnostics indicating near-normal, whitened residuals. **(B) Monthly models:** for *monthly* counts, simple Linear Regression, XGBoost, and LightGBM yield qualitatively reasonable envelopes but do not outperform a monthly naïve baseline; the naïve model attains RMSE = 70.06 (MAE = 59, MSE = 4909), versus 104–207 RMSE for the ML baselines. The workflow delivers visual analytics and forecasts tied directly to GOES flare variables, with SARIMAX supporting cycle turning-point estimates and monthly models serving as cautious envelopes rather than precise long-horizon predictors.

Keywords. Sun: activity, Sun: flares, Sun: X-rays, Sun: statistics, methods: data analysis

1. Introduction

Solar flares are intense bursts of radiation produced by the rapid release of magnetic energy in the solar atmosphere (see, e.g., Tandberg-Hanssen and Emslie 1988; Somov 1991; Svestka 2012; Kowalski 2024). They are primary drivers of space weather, impacting satellites, radio communications, and power systems. Long-term, systematic observations are required to characterize the statistical behavior of flares and to improve forecasting (see, e.g., Temmer 2021; Miteva and Samwel 2022; Gopalswamy 2022).

A large body of work has modeled solar activity as a time series using both linear seasonal models and modern machine-learning regressors (see, e.g., Reikard 2020; Ribeiro and Gradvohl 2021). Seasonal ARIMA/SARIMAX has been applied to the international sunspot number (SSN), sunspot area (SSA), the F10.7 cm flux, and related flare indices (see, e.g., Paraskakis and Hristopulos 2025; Qamar et al. 2025; Bisoi et al. 2024). Tree-based boosting (e.g., XGBoost/LightGBM) has also been explored for non-linear forecasting of SSN and active-region classifications (e.g., Dang et al. 2022; Niu and Huang 2025; Bringewald 2025). Most prior studies rely on century-scale SSN/SSA or region-class catalogs. In contrast, we target the GOES/XRS soft X-ray record directly, forecasting with the *GOES* flare-count and XRS_B flux products used operationally in space-weather monitoring.

© The Author(s), 2026. Published by Cambridge University Press on behalf of The International Astronomical Union.

https://doi.org/10.1017/S1743921326106929 Published online by Cambridge University Press

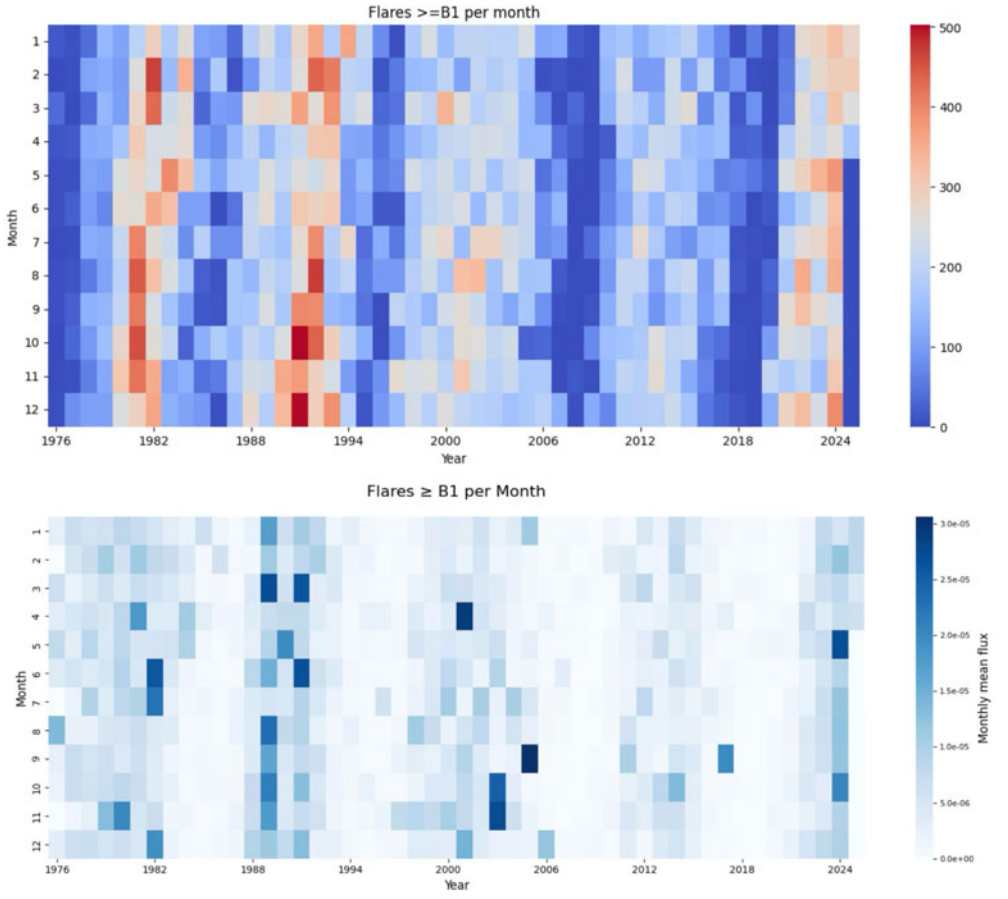


Figure 1. Top: Monthly counts of flares with peak flux $\geq$B1 (GOES 1–8 Å), 1976–2025. **Bottom:** Monthly mean GOES XRS_B flux over the same interval. Both panels highlight the 11-year modulation, extended minima at the cycle boundaries, and the rise of Cycle 25. The count map emphasizes production, while the flux map is more sensitive to months with fewer but brighter events.

Since the 1970s, the Geostationary Operational Environmental Satellites (GOES) have provided a uniquely continuous record of soft X-ray flux, underpinning multi-cycle studies of flare statistics (see, e.g., Janssens et al. 2025; Hudson et al. 2024; Biasiotti and Ivanovski 2025). While the raw data are public, accessible, integrated tools and long-baseline summaries remain valuable for research and education. Here we compile a homogeneous 49-year flare census and introduce an interactive dashboard that enables dynamic exploration of long-term behavior.

2. Data and Methods

2.1. *GOES flare catalog and monthly products*

We use the NOAA/SWPC GOES XRS event list (1–8 Å) from 1976 to April 2025. From this catalog, we derive:

- **Monthly flare counts** for events with peak flux $\geq$B1, and
- **Monthly mean XRS_B flux**, computed as the arithmetic mean of daily means within each month.

https://doi.org/10.1017/S1743921326106929 Published online by Cambridge University Press

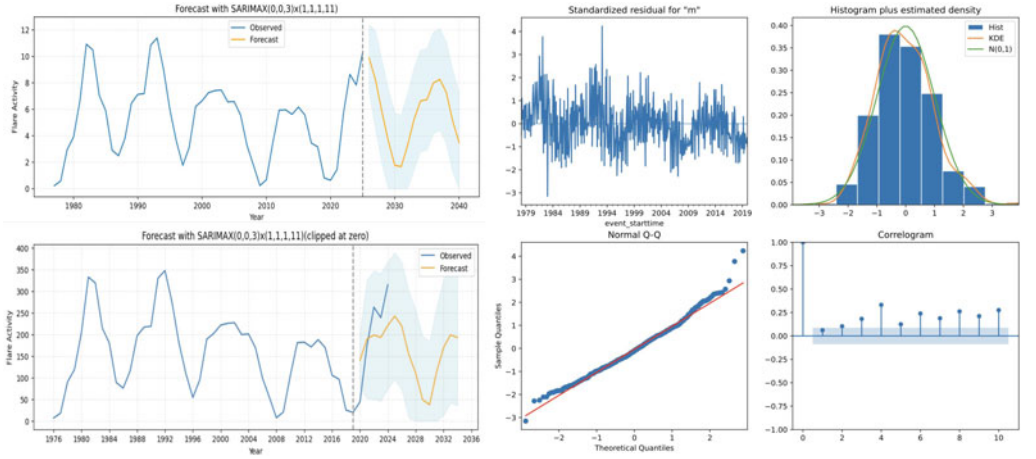


Figure 2. SARIMAX forecasts and diagnostics. **A, B:** Predictions using $(p, d, q) = (0, 0, 3)$ and seasonal $(P, D, Q, s) = (1, 1, 1, 11)$ on two annualized series (daily-mean annual and monthly-mean annual). **C–F:** Standardized residuals, histogram+KDE vs. $\mathcal{N}(0, 1)$, Q–Q, and residual ACF.

These diagnostics appear as Year × Month heat-maps in Fig. 1. In this Figure, both panels exhibit the dominant ∼11-year modulation: activity bands peak during Cycles 21–23 (late 1970s/early 1980s; late 1980s/early 1990s; around 2000) and weaken markedly through Cycle 24, with a renewed rise into Cycle 25 after ∼2023. The *count* map emphasizes how frequently B1+ flares occur, making the prolonged quiet intervals around the Cycle 23/24 minimum particularly evident. In contrast, the *flux* map highlights months when a small number of bright events dominate the monthly mean; isolated darker cells in otherwise moderate years indicate episodes with relatively few but intense flares (e.g., M/X-class clusters). Across years, intra-annual (month-to-month) structure is present, but secondary to the cycle envelope, reinforcing that productivity (counts) and energetics (flux) convey complementary information about flare activity.

2.2. *Forecasting framework: two tracks*

We pursue two complementary tracks and compare each model against a purpose-matched *naïve* baseline defined as simple persistence: the forecast equals the most recently observed value.

(A) Annualized SARIMAX (cycle-scale). Daily counts are aggregated to calendar-year means, $y_t^{\text{annual}} = \frac{1}{N_t} \sum_{d \in \text{year } t} \text{count}_d$, and modeled with $\text{SARIMAX}(0, 0, 3) \times (1, 1, 1)_{11}$. The *annual naïve* baseline is the one-step persistence (previous year):

$$\hat{y}_{t+1}^{\text{naive,ann}} = y_t^{\text{annual}}, \qquad \hat{y}_{t+h}^{\text{naive,ann}} = \hat{y}_{t+h-1}^{\text{naive,ann}} \ (h \geq 2),$$

i.e., a random-walk forecast that repeats the last observed annual value at all future horizons. This is the reference for the annual MSE/MAE figures.

(B) Monthly models (operational cadence). For the *monthly* count series, we evaluate Linear Regression, XGBoost, and LightGBM (lagged features and seasonal dummies) against a *monthly naïve* persistence baseline (the previous month):

$$\hat{y}_{t+1}^{\text{naive,mon}} = y_t^{\text{mon}}, \qquad \hat{y}_{t+h}^{\text{naive,mon}} = \hat{y}_{t+h-1}^{\text{naive,mon}} \ (h \geq 2).$$

This baseline simply carries the last observed monthly value forward. It is the reference for the monthly error results (e.g., RMSE = 70.06, MAE = 59, MSE = 4909).

https://doi.org/10.1017/S1743921326106929 Published online by Cambridge University Press

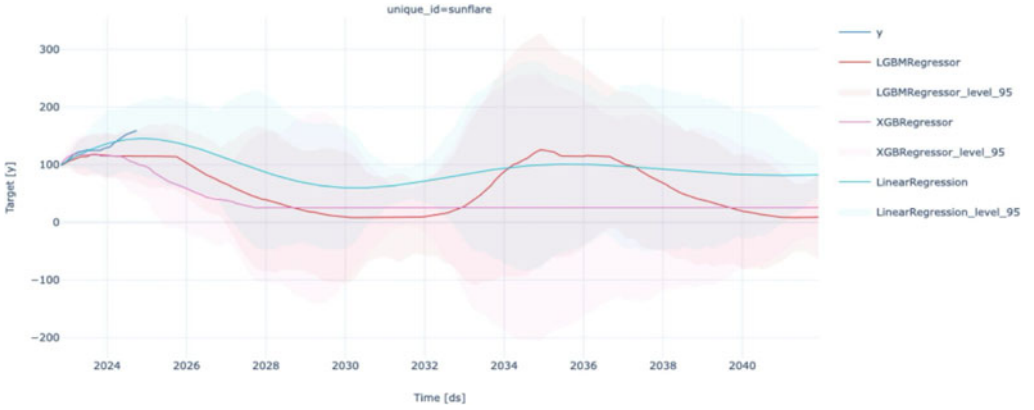


Figure 3. Monthly forecasts of flare counts. Mean trajectories for **Linear Regression** (teal), **LightGBM** (red), **XGBoost** (magenta); shaded bands are nominal 95% intervals. The blue curve shows recent observations.

Evaluation metrics. For both tracks, we report the Mean Absolute Error (MAE), Mean Squared Error (MSE), and Root Mean Squared Error (RMSE); for ML models that emit predictive bands, we also report the empirical coverage of the nominal 95% intervals.

3. Results

3.1. *Forecasting with* annual *SARIMAX and residual diagnostics*

On the annual series, SARIMAX$(0,0,3)\times(1,1,1)_{11}$ improves over an annual naïve seasonal baseline (MSE $= 2.37$ vs. 4.93; MAE $= 1.25$ vs. 1.80), and diagnostics in Fig. 2 indicate approximately normal, whitened errors. Panels **A** and **B** display one-step-ahead fits and multi-year forecasts for the two annualized series (daily-mean annual in A; monthly-mean annual in B). The vertical dashed line marks the train/test split; the blue curve is the observed annual series, and the yellow curve is the SARIMAX mean forecast, with the shaded band denoting the model's approximate 95% predictive interval. In both panels, the forecast reproduces the cycle-scale oscillation with an $\sim$11 yr period and amplitudes comparable to recent cycles; the band widens steadily with horizon, as expected. In **B**, the series is non-negative by construction, and forecasts are shown *clipped at zero*, which makes the lower predictive band asymmetric near minima.

Panels **C**-**F** in Fig. 2 summarize the residual diagnostics from the fitted model. The **standardized residuals over time** (**C**) are centered near zero, with no visible long-term drift or heteroscedastic episodes. The **histogram with KDE and** $\mathcal{N}(0,1)$ **reference** (**D**) shows a distribution close to Gaussian, with only mild tail deviations. The **normal Q–Q plot** (**E**) follows the 45° line through the bulk of the data; slight curvature at the extremes indicates modest non-Gaussian tails that are typical for annualized solar activity. Finally, the **residual ACF** (**F**) lies within the 95% bounds at most lags, with no significant spikes, supporting the interpretation that the remaining autocorrelation has been largely removed by the $(0,0,3)\times(1,1,1)_{11}$ structure.

Turning-point estimates from the annualized fit are: **Cycle 25 minimum** $\sim$2030 (amplitude 1.67; 95% CI: 0.00-5.56), **Cycle 26 maximum** $\sim$2036 (8.26; 4.43-12.10), and **Cycle 26 minimum** $\sim$2041 (1.45; 0.00-5.24).

3.2. *Forecasting with* monthly *models*

The short blue segment in Fig. 3 at the far left marks the most recently observed months used for validation. The **Linear Regression** trajectory (teal) projects a gradual

https://doi.org/10.1017/S1743921326106929 Published online by Cambridge University Press

decline from present levels into a broad trough near ∼2029–2031, followed by a slow recovery toward the mid-2030s; its band is comparatively tight early on and widens smoothly with the horizon. **LightGBM** (red) dips more sharply to a deeper minimum around ∼2031–2033 and then rebounds to a crest near ∼2034–2036 before declining again, illustrating sensitivity to non-linear interactions among lags; its nominal 95% band is narrow but, as discussed below, under-dispersed. **XGBoost** (magenta) stays close to a near-flat baseline with a slight downward drift through the early 2030s, reflecting a conservative fit under the available features. Across all models, the shaded uncertainty grows rapidly beyond ∼1–2 yr, and the three mean paths loosely converge around ∼2034 at moderate activity before diverging again at longer horizons.

Across models, monthly predictive bands widen rapidly beyond ∼1–2 yr. In our 90:10 split, Linear Regression, XGBoost, and LightGBM produce RMSE values of ∼105, 116, and 207, respectively, with coverage near 100% (Linear) and under-dispersion for the boosted trees (coverage ∼10% and ∼2%). By contrast, the **monthly naïve** baseline achieves $\mathbf{MAE} = 59$, $\mathbf{MSE} = 4909$, and $\mathbf{RMSE} = 70.06$, outperforming all three monthly ML models in RMSE (and MAE, where comparable). Thus, while monthly ML provides useful qualitative envelopes and scenario diversity, the naïve model remains the most competitive quantitative baseline at a monthly cadence for this record length and feature set.

4. Conclusion and Outlook

We presented GOES/XRS visual analytics and two forecasting tracks tied directly to flare variables. The monthly heat-maps (counts and mean XRS_B) separate *productivity* from *energetics* and make the cycle envelope, extended minima, and the rise of Cycle 25 visually explicit. On an *annualized* series, a parsimonious $\mathrm{SARIMAX}(0,0,3) \times (1,1,1)_{11}$ improves over an annual seasonal naïve baseline (MSE 2.37 vs. 4.93; MAE 1.25 vs. 1.80) with residuals that are close to Gaussian and largely whitened; it yields interpretable turning-point estimates–Cycle 25 minimum ∼2030, Cycle 26 maximum ∼2036, and Cycle 26 minimum ∼2041 (with associated uncertainty bands)–showing that, after annualization, cycle-scale structure is strong enough for SARIMAX to add skill beyond simple recurrence. For the *monthly* count series, Linear Regression, XGBoost, and LightGBM produce plausible envelopes but do not surpass a monthly seasonal naïve baseline (RMSEs 70.06, MAE 59, MSE 4909); in our 90:10 split, the ML models achieve RMSEs of ∼105 (Linear), 116 (XGBoost), and 207 (LightGBM), with boosted trees exhibiting under-dispersed uncertainty. Overall, cycle-scale prediction benefits from aggregation and a simple, interpretable structure, whereas monthly horizons remain data-limited; sunspot area/number series–available for centuries–are therefore attractive exogenous drivers because they expand the effective training baseline and can stabilize monthly forecasts.

Acknowledgements

Buitrago-Casas's work was supported by the NASA Early Career Investigator Program (ECIP), award **80NSSC23K1063**, project *"Real-Time Flare Onset Alert"*.

References

Lorenzo Biasiotti and Stavro Lambrov Ivanovski. Statistical analysis of solar flare properties from 1975 to 2017. *Solar Physics*, 300(8):121, 2025.

Susanta Kumar Bisoi, Mayank Rajput, P Janardhan, Y Siva Kumar, and Sibaram Panigrahi. Prediction of solar cycle 25 using f10. 7 cm radio flux and machine learning techniques. 2024.

Julia Bringewald. Solar flare forecast: A comparative analysis of machine learning algorithms for solar flare class prediction. *arXiv preprint arXiv:2505.03385*, 2025.

https://doi.org/10.1017/S1743921326106929 Published online by Cambridge University Press

Yuchen Dang, Ziqi Chen, Heng Li, and Hai Shu. A comparative study of non-deep learning, deep learning, and ensemble learning methods for sunspot number prediction. *Applied Artificial Intelligence*, 36(1):2074129, 2022.

Nat Gopalswamy. The sun and space weather. *Atmosphere*, 13(11):1781, 2022.

Hugh Hudson, Ed Cliver, Stephen White, Janet Machol, Courtney Peck, Kim Tolbert, Rodney Viereck, and Dominic Zarro. The greatest goes soft x-ray flares: Saturation and recalibration over two hale cycles. *Solar Physics*, 299(3):39, 2024.

Jan Janssens, Véronique Delouille, Frédéric Clette, and Jesse Andries. Solar flare rates and probabilities based on the mcintosh classification: Impacts of goes/xrs rescaling and revisited sunspot classifications. *Journal of Space Weather and Space Climate*, 15:14, 2025.

Adam F Kowalski. Stellar flares. *Living Reviews in Solar Physics*, 21(1):1, 2024.

Rositsa Miteva and Susan W Samwel. M-class solar flares in solar cycles 23 and 24: properties and space weather relevance. *Universe*, 8(1):39, 2022.

B Niu and Z Huang. Multi-step probabilistic forecasting for sunspot numbers based on lightgbm. *Advances in Space Research*, 2025.

Nikolaos Paraskakis and Dionissios T Hristopulos. Prediction of yearly mean sunspot number using machine learning methods. *Stochastic Environmental Research and Risk Assessment*, pages 1–28, 2025.

Waqas Qamar, Majid Hussain, M Basit Zaheer, Jawaid Akram, Naeem Sadiq, and Zaheer Uddin. Prediction of sunspot numbers via weibull distribution and deep learning. *Astrophysics and Space Science*, 370(7):1–9, 2025.

Gordon Reikard. Forecasting long-term solar activity with time series models: Some cautionary findings. *Journal of Atmospheric and Solar-Terrestrial Physics*, 211:105465, 2020.

Fernanda Ribeiro and André Leon S Gradvohl. Machine learning techniques applied to solar flares forecasting. *Astronomy and Computing*, 35:100468, 2021.

Boris V Somov. *Physical processes in solar flares*, volume 172. Springer Science & Business Media, 1991.

Zdenek Svestka. *Solar flares*, volume 8. Springer Science & Business Media, 2012.

Einar Tandberg-Hanssen and A Gordon Emslie. *The physics of solar flares*, volume 14. Cambridge University Press, 1988.

Manuela Temmer. Space weather: The solar perspective: An update to schwenn (2006). *Living Reviews in Solar Physics*, 18(1):4, 2021.

https://doi.org/10.1017/S1743921326106929 Published online by Cambridge University Press